

An FSO-based Drone Assisted Mobile Access Network for Emergency Communications

Di Wu, *Student Member, IEEE*, Xiang Sun, *Member, IEEE*, and Nirwan Ansari, *Fellow, IEEE*

Abstract—Deploying drone mounted base stations (DBSs) can quickly recover communications of mobile users (MUs) in a disaster struck area. That is, DBSs can act as relay nodes to transmit data from remote working base stations (which are located out of the disaster struck area) to MUs. Since DBSs could be deployed very close to MUs, the access link data rates between DBSs and MUs are well provisioned. However, DBSs may be far away from the remote working base stations, and thus the backhaul link data rate between a DBS and the remote working base station could be throttled. Free Space Optics (FSO), which has been demonstrated to provision high speed point-to-point wireless communications, can be leveraged to improve the capacity of the backhaul link. Since FSO requires line-of-sight between a DBS and a remote working macro base station, DBSs have to be carefully deployed. In this paper, we design a QoS aware drone base Station placement and mobile User association strategy (RESCUE) in the context of FSO based drone assisted mobile access networks to jointly optimize the DBS deployment, MU association, and bandwidth allocation such that the number of the served MUs in the disaster struck area is maximized. The performance of RESCUE is validated via extensive simulations.

Index Terms—Drone-mounted base station, free space optics, drone deployment, disaster

I. INTRODUCTION

Owing to the high availability and high data rate provided by mobile networks, the number of mobile subscribers is increasing over the years [1]. According to Ericsson Mobility Report [2], the total number of mobile subscriptions was around 7.9 billions in Q3 2018 and was forecast to reach 8.9 billions by the end of 2024. However, the mobile network infrastructure, such as base stations (BSs) and power transmission lines (which transport electricity from the power grid to BSs), could be damaged owing to natural disasters. Consequently, mobile users (MUs) in a disaster struck area (i.e., the area covered by malfunctioned BSs) are unable to connect to the network and obtain any services. How to quickly recover communications in the disaster struck area is a very critical issue which has drawn much attention [3]. Quickly recovering communications can help people in disaster struck areas transmit the disaster information out of the area. Thus, rescue personnel can make accurate evaluation of disasters and design efficient rescue plans [4]–[6]. In rescuing people afflicted by disasters, valid

wireless communications can help reduce the searching area and enhance survivability [7].

There are many strategies to recover communications in disaster struck areas. One method is to equip ground vehicles with radio head to conduct the function of ground movable BSs. Ground movable BSs can be deployed near the disaster struck area to provision MUs with temporary communications by forwarding data between MUs and nearby working macro BSs (MBSs), which are located in the disaster struck area; also, ground movable BSs can move to different locations upon requests [8], [9]. The drawbacks of applying ground movable BSs, however, include 1) **inefficient deployment**: deploying a ground movable BS to a designated destination may not always be feasible as the road to the designated destination may be damaged; 2) **limited wireless backhaul capacity**: the deployed ground movable BS is considered as a relay node between MUs and a specific working MBS. The ground movable BS can be deployed in the disaster struck area close to MSs, but the distance between a ground movable BS and a working MBS could be very long [10]–[12]. Also, the link between a working MBS and a ground movable BS may likely be on Non-Line of Sight (NLoS). Consequently, the pathloss between the ground movable BS and the working MBS may be very high, thus limiting the wireless backhaul (between a ground movable BS and a working MBS) capacity. Note that the limited backhaul capacity may stifle the ground movable BS from relaying traffic from MUs to working MBSs.

In order to overcome the inefficient deployment and limited wireless backhaul capacity problem in the ground movable BSs strategy, drone mounted base stations (DBSs), which act as relay nodes between MUs and working MBSs [13]–[15], can be deployed over the disaster struck area. Different from ground movable BSs, DBSs can move in the air, and so can be deployed over the designated destination efficiently and flexibly [16]–[18]. Also, a DBS can hover at a high altitude to facilitate Line of Sight (LoS) for the wireless backhaul link between the DBS and its working MBS, thus potentially reducing the pathloss between the DBS and its working MBS and increasing wireless backhaul capacities [19]. However, the wireless backhaul capacity is still very limited owing to the long distance between a DBS and its working MBS [20]. Also, the DBS can ferry traffic back to the working MBS. That is, a drone collects data from MUs, flies back to the working MBS, and transmits the collected data to the working MBS [21]. This method mitigate the limited wireless backhaul capacity constraint, but incurs a long communications delay caused by the latency of the DBS flying back to the working MBS.

In order to quickly recover communications in disaster

D. Wu and N. Ansari are with Advanced Networking Lab., Department of Electrical & Computer Engineering, New Jersey Institute of Technology, Newark, NJ 07102, USA. E-mail: {dw245, nirwan.ansari}@njit.edu.

X. Sun is with Smart Edge Computing and Networking Lab., Department of Electrical & Computer Engineering, University of New Mexico, Albuquerque, NM 87131, USA. E-mail: sunxiang@unm.edu.

This work is supported by the National Science Foundation under Award CNS-1814748 and OIA-1757207.

struck areas and achieve low communications delay between MUs and working MBSs, we propose the free space optics (FSO) based drone assisted mobile access network architecture. As shown in Fig. 1, a number of DBSs¹ can be quickly deployed over the disaster struck area. MUs in the disaster struck area will associate to a specific DBS, which relays traffic between the nearby working MBS and associated MUs. Here, the access links between MUs and their DBS are using radio frequency (RF) communications, and the backhaul link between the DBS and its working MBS is applying FSO communications. Note that FSO communications is a point-to-point wireless communications technology that can achieve a very high throughput over a long distance [22], [23]. Applying FSO as wireless backhaul communications can dramatically increase the network capacity, and thus significantly reduce the delay of transmitting data between MUs and working MBS via DBSs [24].

The contributions of this paper are summarized as follows. 1) The FSO based drone assisted mobile access network architecture is proposed to quickly recover communications in the disaster struck area and achieve low network delays between MUs in disaster struck areas and working MBSs, which are located out of disaster struck areas. 2) The "QoS aWare drone base Station plaCement and mobile User association stratEgy (RESCUE)" algorithm is proposed in the context of the FSO based drone assisted mobile access network architecture to determine the network parameters (i.e., the 3-D locations of DBSs, the MU association, and the bandwidth allocation in access links) in order to maximize the number of served MUs, which is defined as the number of MUs with guaranteed data rate requirements (traffic from the nearby MBSs to the MUs via the DBSs). 3) The performance of RESCUE is validated via extensive simulations.

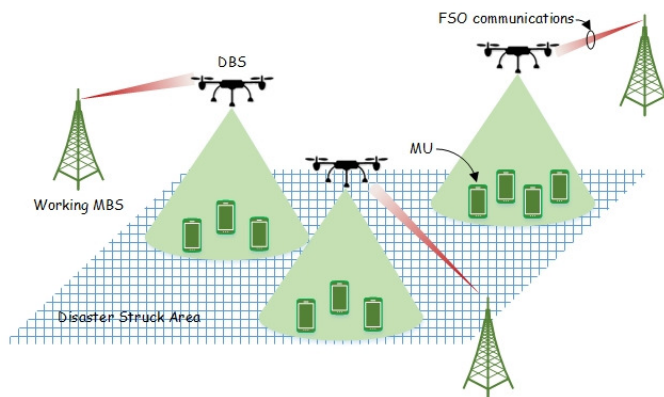


Fig. 1. FSO based drone assisted mobile access network architecture.

The rest of this paper is organized as follows. In Section II, we compare the related works. In Section III, we introduce the architecture of DBS assisted emergency communications in

disaster struck areas with FSO backhaul links. The problem of maximizing the number of MUs served by DBSs in a disaster struck area is formulated in Section IV. Our proposed heuristic algorithm to solve this problem is discussed in Section V and the simulation results are analyzed in Section VI. A brief conclusion is drawn in Section VII.

II. RELATED WORKS

Applying DBSs to assist mobile access networks in delivering traffic to MUs has received much attention. Sun and Ansari [25] proposed to deploy a DBS over a hotspot area to facilitate content delivery from an MBS to MUs via the DBS by jointly optimizing the DBS placement and user association to maximize the overall spectral efficiency of the hotspot area. Yaliniz *et al.* [26] proposed a DBS placement problem to determine the altitude and the user association area of a DBS such that the DBS can cover as many MUs as possible, while satisfying the QoS requirements (in terms of the pathloss from the DBS to an MU being less than a predefined threshold) for each MU, which is associated to the DBS. Rather than placing one DBS, Zhang *et al.* [27] proposed to deploy multiple DBSs over a hotspot area. They developed a strategy of deploying multiple DBSs in the 3-D space over a given hotspot area in order to minimize the number of deployed DBSs while guaranteeing QoS requirements (in terms of pathloss requirements) of all the MUs in the hotspot area.

Applying drones to help MUs communicate with base stations in a disaster scenario has been investigated. Erdelj *et al.* [28] exploited on drones assisted wireless sensor networks to facilitate disaster management, which covers three stages, i.e., disaster prediction, assessment, and response. Narang *et al.* [29] deployed a drone ad-hoc network over a disaster struck area, where the access points near the disaster struck area could deliver traffic to MUs via the established drone ad-hoc network in a multi-hop manner. They designed a drone deployment algorithm to optimize the locations of drones in order to maximize the throughput of the drone ad hoc network. Hayajneh *et al.* [30] assumed that MUs in a disaster struck area tend to cluster in a number of hotspot areas. Based on this assumption, a number of drones are deployed over each hotspot. They evaluated how the number of drones deployed in a hotspot and the configurations of each drone (i.e., the location and the transmission power of a drone) affect the coverage probability and the average energy efficiency in downloading data from drones to MUs.

On the other hand, FSO communications has been proved to provision a high speed point-to-point communications [22] [23], and integrating drones into the FSO system has been explored. Fawaz *et al.* [31] proposed a drone assisted FSO relay system, where a drone equipped with an FSO transceiver is considered as a relay node to relay the FSO beam between an FSO transmitter and an FSO receiver. The drone assisted FSO relay system may reduce the atmosphere attenuation of the FSO link, especially when the distance between the FSO transmitter and the FSO receiver is very long. Applying FSO and drones as the front-hauling/back-hauling technology in mobile networks has recently been proposed [32], where

¹Note that the limited flying time of a battery-powered drone could be the major roadblock of deploying DBSs in the disaster struck area. However, the flying time can be extended by applying gasoline-powered drones (which can last nearly one hour and get a fast refuel) or applying more than one drones to serve a group of MUs. For example, we can use two drones iteratively serving the same MUs.

geographically distributed base stations are connected to their nearby drones (which are hovering in the air) via FSO communications, and those drones cooperate with each other to establish an FSO based drone ad-hoc network, which is to deliver the traffic between the mobile core network and distribution BSs. FSO communications between different drones is deployed in the drone ad-hoc network. Based on the proposed FSO based drone ad-hoc network, Gu *et al.* [33] designed a network topology reconfiguration method to dynamically adjust the FSO connections among different drones based on the traffic demands of different BSs to enhance the throughput of the drone ad-hoc network. Najafi *et al.* [34] applied a drone to relay traffic from users to the central unit, where the drone is equipped with a RF module and an FSO transmitter. The access link (between the drone and the users) applies RF communications (e.g., sub-6 GHz RF communications) and the fronthaul link (between the drone and the central unit) applies the FSO link. They investigated the geometric loss of the FSO link owing to the random fluctuation of the position and orientation of the hovering drone.

FSO communications has been proposed to be utilized in mobile networks; here, we focus on how to deploy DBSs using FSO as backhaul links between DBSs and MBSs in disaster struck areas. As mentioned before, using FSO communications and DBSs can quickly establish network connections to MUs in disaster struck areas in carrying out emergency rescue.

III. SYSTEM MODEL

Denote I as the set of DBSs being deployed in the disaster struck area, and $i \in I$ is used to index these DBSs. Denote J as the set of MUs in the disaster struck area, and $j \in J$ is used to index these MUs. Let a_{ij} be the binary variable to indicate whether MU j is served by DBS i (i.e., $a_{ij} = 1$) or not (i.e., $a_{ij} = 0$).

A. Average pathloss between a DBS and an MU

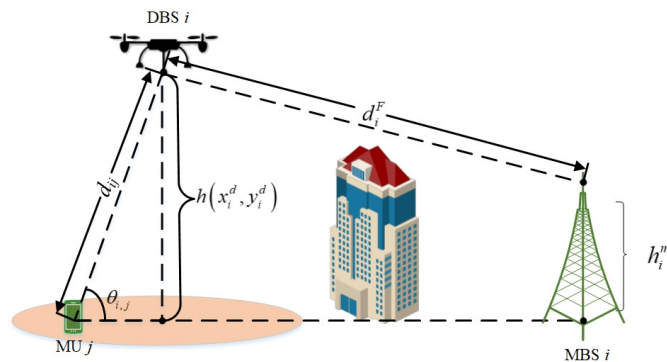


Fig. 2. Pathloss Model.

The communications channel between an MU and its associated DBS is normally modeled as a probabilistic Line-of-Sight (LoS) channel. Denote the pathloss between DBS i and MU j (in dB) in LoS and NLoS as η_{ij}^{LoS} and η_{ij}^{NLoS} , respectively, where [35]

$$\eta_{ij}^{LoS} = 20 \log \left(\frac{4\pi f_c d_{ij}}{c} \right) + \xi^{LoS}, \quad (1)$$

$$\eta_{ij}^{NLoS} = 20 \log \left(\frac{4\pi f_c d_{ij}}{c} \right) + \xi^{NLoS}, \quad (2)$$

where ξ^{LoS} and ξ^{NLoS} stand for the average value of excessive pathloss² in LoS and NLoS, respectively, f_c is the carrier frequency, c is the speed of light, and d_{ij} is the distance between DBS i and MU j . As illustrated in Fig. 2, d_{ij} can be calculated by

$$d_{ij} = \sqrt{(x_i^d - x_j)^2 + (y_i^d - y_j)^2 + h^2(x_i^d, y_i^d)}. \quad (3)$$

Here, $h(x_i^d, y_i^d)$ is the altitude of DBS i when DBS i is deployed at the horizontal location $\langle x_i^d, y_i^d \rangle$, and $\langle x_j, y_j \rangle$ indicates the horizontal location of MU j . The horizontal distance between MU j and DBS i is denoted by l_{ij}

$$l_{ij} = \sqrt{(x_i^d - x_j)^2 + (y_i^d - y_j)^2}. \quad (4)$$

The probability of having LoS between DBS i and MU j (ρ_{ij}) is

$$\rho_{ij} = \frac{1}{1 + be^{-\beta(\theta_{ij}-b)}}, \quad (5)$$

where b and β are the two environmental parameters in the disaster struck area, and θ_{ij} is the elevation angle between DBS i and MU j (as indicated in Fig. 2), i.e.,

$$\theta_{ij} = \arcsin \left(\frac{h(x_i^d, y_i^d)}{d_{ij}} \right). \quad (6)$$

Based on Eq. (5) and Eq. (6), we can derive that DBS i with a higher altitude leads to a larger value of elevation angle, thus incurring a higher probability of having an LoS link to MU j .

The average pathloss between DBS i and MU j , denoted as $\bar{\eta}_{ij}$, can be modeled as [36]

$$\bar{\eta}_{ij} = \rho_{ij}\eta_{ij}^{LoS} + (1 - \rho_{ij})\eta_{ij}^{NLoS}. \quad (7)$$

Note that DBS i can communicate with MU j if the average pathloss between MU j and DBS i is larger than a predefined threshold η^{th} . Thus, the horizontal distance between DBS i and MU j is maximized when

$$\bar{\eta}_{ij} = \eta^{th}. \quad (8)$$

Definition 1. The optimal elevation angle between DBS i and MU j is defined as the elevation angle between DBS i and MU j that maximizes the horizontal distance between DBS i and MU j .

In order to find the optimal elevation angle (denoted as θ_{ij}^*), we can take the derivative of η^{th} with respect to θ_{ij} . By letting $\frac{\partial \bar{\eta}_{ij}}{\partial \theta_{ij}} = 0$, we can find θ_{ij}^* such that:

$$\frac{\pi}{9 \ln(10)} \tan \theta_{ij}^* + \frac{b\beta (\eta_{ij}^{LoS} + \eta_{ij}^{NLoS}) e^{(-\beta(\theta_{ij}^*-b))}}{(be^{(-\beta(\theta_{ij}^*-b))} + 1)^2} = 0 \quad (9)$$

Definition 2. The optimal altitude of DBS i is defined as the altitude of DBS i that maximizes the horizontal distance between DBS i and MU j .

²Excessive pathloss is the additional pathloss on top of the free space pathloss incurred between a DBS and an MU.

The optimal elevation angle θ_{ij}^* , which maximizes the horizontal distance between DBS i and MU j , can be derived by solving Eq. (9). By substituting $\theta_{ij} = \theta_{ij}^*$ into Eq. (8), we can derive the related maximum horizontal distance between DBS i and MU j , denoted as l_{ij}^{max} . Thus, the optimal altitude of DBS i is

$$h_{ij}^* = l_{ij}^{max} \tan \theta_{ij}^*. \quad (10)$$

Intuitively, the communication coverage of DBS i is maximized if DBS i is deployed at its optimal altitude.

B. Data rate model of wireless access link

As mentioned earlier, multiple DBSs are deployed in the disaster struck area. Each DBS is associated with its nearby MBS, and thus the DBS can download traffic from the MBS and relay them to MUs. Different DBSs use different spectrum bands to relay traffic to their MUs, and thus there is no interference among MUs in downloading traffic from their DBSs. Denote B_i as the total available bandwidth for DBS i in transmitting traffic to associated MUs, and b_{ij} is used to represent the amount of bandwidth allocated for MU j in downloading traffic from DBS i . Thus, we can obtain the data rate of MU j in downloading traffic from DBS i (denoted as r_{ij}) as

$$r_{ij} = b_{ij} \log \left(1 + \frac{P_i 10^{-\bar{\eta}_{ij}/10}}{N_0} \right), \quad (11)$$

where P_i indicates the transmission power of DBS i . Note that we only consider the downlink scenario in this work because the downlink traffic is much heavier than the uplink traffic (note that the ratio of downlink to uplink traffic is 6:1 [37]).

C. Data rate model of FSO backhaul link

FSO communications is applied to enable DBSs in downloading traffic from nearby MBSs. The data rate model of the FSO link between DBS i and its MBS can be modeled as³ [38]

$$R_i = \frac{P_t}{E_p N_b} \frac{r_s^2}{(\theta_g d_i^F/2)^2} \eta_t \eta_r 10^{-e^{\sigma d_i^F}}, \quad (12)$$

where N_b is the sensitivity of the receiver (photons/bit); E_p is the energy of each photon, i.e., $E_p = h_p c / \lambda$ (here, h_p is the Planck's constant, c is the light speed, and r_s is the radius of the FSO beam at the DBS i 's associated MBS); θ_g is the divergence angle of the optical beam; η_t is the coefficient to convert electrical energy into optical energy at the DBS i 's associated MBS; η_r is the coefficient to convert optical energy into electrical energy at DBS i ; d_i^F is the distance between DBS i and its associated MBS, i.e.,

$$d_i^F = \sqrt{(h(x_i^d, y_i^d) - h_i^m)^2 + (x_i^d - x_i^m)^2 + (y_i^d - y_i^m)^2}, \quad (13)$$

where $\langle x_i^m, y_i^m, h_i^m \rangle$ indicates the 3-D location of DBS i 's associated MBS; σ in Eq. (12) is the atmospheric attenuation coefficient, given by [39] as

$$\sigma = \frac{3.91}{v} \left(\frac{\lambda}{550} \right)^{-q} \quad (14)$$

³We assume that the Acquisition, Tracking, and Pointing (ATP) system is applied, and thus the pointing loss is considered.

where v is the visibility (the maximum distance that one object can be clearly discerned). Denote q as the size distribution of the scattering particles. The relationship between q and v is given by [39]

$$q = \begin{cases} 1.6, & v > 50, \\ 1.3, & 6 < v \leq 50, \\ 0.16v + 0.34, & 1 < v \leq 6, \\ v - 0.5, & 0.5 < v \leq 1, \\ 0, & v \leq 0.5, \end{cases} \quad (15)$$

where the value of v depends on the weather conditions. For example, $v > 50$ when weather is a clear sky, $1 < v \leq 6$ for a hazy weather, and $v \leq 1$ for foggy weather.

IV. PROBLEM FORMULATION

Assume that the number of available DBSs is predetermined. These DBSs will be deployed to help the MUs in the disaster struck area download data from nearby MBSs. We assume that each MBS is only equipped with one FSO transceiver, and thus can only communicate with one DBS. Denote a_{ij} as the binary variable to indicate whether MU j is associated with DBS i (i.e., $a_{ij} = 1$) or not (i.e., $a_{ij} = 0$). We formulate the DBS configuration and MUs association problem to determine the 3-D locations of DBSs, MUs association, as well as the bandwidth allocation to different MUs in order to maximize the number of satisfied MUs⁴ (i.e., their QoS in terms of data rate requirements is met). That is,

$$\mathbf{P0}: \arg \max_{x_i^d, y_i^d, h(x_i^d, y_i^d), a_{ij}} \sum_{i \in I} \sum_{j \in J} a_{ij}, \quad (16)$$

$$\text{s.t. : } C1: \sum_{i \in I} a_{ij} \leq 1, \quad \forall j \in J, \quad (17)$$

$$C2: f^{min}(x_i^d, y_i^d) \leq h(x_i^d, y_i^d) \leq f^{max}(x_i^d, y_i^d), \quad (18)$$

$$C3: a_{ij}(\eta_{ij} - \eta_{ij}^{th}) \leq 0, \quad \forall j \in J, \quad \forall i \in I, \quad (19)$$

$$C4: a_{ij}(r_{ij} - r_j^{th}) \geq 0, \quad \forall i \in I, \quad \forall j \in J, \quad (20)$$

$$C5: \sum_{j \in J} a_{ij} r_{ij} \leq R_i, \quad \forall i \in I, \quad (21)$$

$$C6: \sum_{j \in J} a_{ij} b_{ij} \leq B_i, \quad \forall i \in I, \quad (22)$$

where Constraint C1 ensures that each MU is served by at most one DBS; Constraint C2 imposes the altitude constraints of deploying a DBS, where $f^{min}(x_i^d, y_i^d)$ implies the minimum altitude of DBS i to maintain the LoS between DBS i and its associated MBS if DBS i is deployed at $\langle x_i^d, y_i^d \rangle$, and $f^{max}(x_i^d, y_i^d)$ is the maximum altitude that DBS i can reach. Constraint C3 indicates that MU j can be associated with DBS i (i.e., $a_{ij} = 1$) if the pathloss between MU j and DBS i is not larger than the threshold η^{th} (i.e., $\eta_{ij} - \eta^{th} \leq 0$). Constraint C4 implies that QoS in terms of the data rate requirement of

⁴In the disaster struck area, the mobile network infrastructure may be damaged, and thus MUs are unable to communicate with others, such as the first response team and their families. Establishing emergence communications is very critical for MUs in the disaster struck area. For example, reporting the locations of MUs (by sending short messages) to the first response team can facilitate the rescue. Here, sending short messages does not require a high data rate. Thus, enabling more MUs to be able to communicate with the first response team is considered as the ultimate objective.

TABLE I
LIST OF PARAMETERS

I	Set of all available DBSs
J	Set of all MUs
i	Index of DBSs ($i \in I$)
j	Index of MUs ($j \in J$)
a_{ij}	Binary variable to indicate the user association
x_i^d, y_i^d	Horizontal location of DBS i
x_i^m, y_i^m	Horizontal location of DBS i 's associated MBS
x_j, y_j	Horizontal location of MU j
d_{ij}	Horizontal distance between DBS i and MU j
$h(x_i^d, y_i^d)$	Altitude of DBS i if DBS i is over location (x_i^d, y_i^d)
$f^{max}(x_i^d, y_i^d)$	Maximum altitude of a DBS at location (x_i^d, y_i^d)
$f^{min}(x_i^d, y_i^d)$	Minimum altitude of a DBS at location (x_i^d, y_i^d)
η_{ij}	Average pathloss between DBS i and MU j
η^{th}	Average pathloss threshold
h_i^m	Altitude of MBS i
r_{ij}	Downloading data rate from DBS i to MU j
r_j^{th}	Downloading data rate requirement of MU j

MU j (denoted as r_j^{th}) should be satisfied if it is associated with DBS i ; Constraint C5 implies that the data rate of the backhaul link between DBS i and its associated MBS should be no less than the data rate of the access link for DBS i (which is equal to the sum of all the data rates of the MUs associated with DBS i). Essentially, Constraint C5 ensures that the backhaul link is not the bottleneck. Constraint C6 ensures the total bandwidth allocated to MUs by each DBS is within the total bandwidth it can use.

V. QoS AWARE DBS PLACEMENT AND MU ASSOCIATION ALGORITHM

We propose a heuristic algorithm, i.e., QoS aware drone base Station placement and mobile User association strategy (RESCUE), to efficiently solve **P0**. The basic idea of RESCUE is to decompose **P0** into two sub-problems, i.e., DBS placement and bandwidth allocation. By solving the two sub-problems iteratively, RESCUE can achieve a near optimal solution of **P0**. RESCUE is summarized in Algorithm 1.

Initial 3-D DBS placement: The disaster struck area is first divided into a number of locations with the same size. Denote the set of these locations as N . So, if DBS i is placed over location n (where $n \in N$), then the 2-D coordinate of DBS i (i.e., (x_i^d, y_i^d)) equals to the center of location n , and DBS i will connect to the closest MBS to download traffic. The objective of the initial 3-D DBS placement is to find the optimal location where DBS i can cover the maximum number of the MUs (which are not associated with other deployed DBSs)⁵. Denote J' as the set of MUs that are not associated with any deployed DBSs (i.e., $J' = \{j \in J | a_{ij} = 0, \forall i \in I\}$), and $J' = J$ when we deploy the first DBS. In order to find the optimal location with respect to DBS i , we will iteratively place DBS i over each location in the disaster struck area and select the one which can cover the maximum number of MUs. Specifically,

- 1) Select location n and place DBS i over location n . Based on **Definition 2**, the optimal altitude of DBS

i that maximizes the coverage area can be obtained by Eq. (10), i.e., $h(x_i^d, y_i^d) = h_i^*$. Note that, in order to satisfy C2 in **P0**, $h(x_i^d, y_i^d) = f^{min}(x_i^d, y_i^d)$, if $h_i^* < f^{min}(x_i^d, y_i^d)$ and $h(x_i^d, y_i^d) = f^{max}(x_i^d, y_i^d)$, if $h_i^* > f^{max}(x_i^d, y_i^d)$.

- 2) After having determined the altitude of DBS i at location n , we calculate the average pathloss between DBS i and all the MUs in J' and check if these MUs can be covered by DBS i or not. Denote K_{in} as the set of MUs that can be covered by DBS i deployed over location n , i.e., $K_{in} = \{j \in J' | \eta_{ij} \leq \eta^{th}\}$, and $|K_{in}|$ is used to indicate the number of MUs covered by DBS i .
- 3) We iteratively select a location in the disaster struck area and derive the number of MUs that can be covered by DBS i , i.e., the value of $|K_{in}|$ (where $n \in N$), based on the previous two steps. Thus, the optimal location of DBS i is the location that incurs the largest value of $|K_{in}|$, i.e., $n_i^* = \arg \max\{|K_{in}| | n \in N\}$. Therefore, DBS i will be placed over the center of location n^* .

Bandwidth allocation and MU association: After having determined the 2-D location of DBS i , each MU covered by DBS i should be allocated sufficient bandwidth to satisfy its data rate requirement (i.e., C4 in **P0**). Here, we define the bandwidth requirement of MU j as the minimum amount of bandwidth that meets the data rate requirement of MU j , i.e.,

$$b_{ij} = \frac{r_{ij}}{\log \left(1 + \frac{P_i 10^{-\eta_{ij}/10}}{N_0} \right)}. \quad (23)$$

However, the total amount of available bandwidth of DBS i (i.e., B_i) is limited, and so not all the MUs covered by DBS i can be allocated sufficient bandwidth to meet their data rate requirements. In order to maximize the number of the MUs (such that their data rate requirements are met), DBS i will first allocate bandwidth to the MU, which incurs the least bandwidth requirement⁶. Specifically,

- 1) Construct an array by sorting all the MUs covered by DBS i (i.e., $\forall j \in K_{in^*}$) in ascending order according to their bandwidth requirements (b_{ij}). Assume that MU j' is the first MU in the array. Allocate $b_{ij'}$ amount of bandwidth to MU j' , associate MU j' to DBS i , i.e., $a_{ij'} = 1$, and update the available bandwidth of DBS i by $B_i = B_i - b_{ij'}$.
- 2) Select the next MU in the array, allocate the required bandwidth to the MU, and associate the MU to DBS i . The iteration continues until all the MUs covered by DBS i are associated to DBS i (i.e., $\forall j \in K_{in^*}, a_{ij} = 1$), or DBS i does not have enough bandwidth to meet the bandwidth requirement of the selected MU, or the overall data rate between the associated MUs and DBS i exceeds the capacity of the FSO backhaul link between DBS i and its connected MBS (i.e., C5 in **P0**).

Altitude adjustment: when DBS i is unable to meet the data rate requirements of some MUs covered by DBS i because of the limited available bandwidth of DBS i (i.e., B_i),

⁵Note that an MU is covered by a DBS implies that the pathloss between the MU and the DBS is no larger than the pathloss threshold η^{th} .

⁶The required bandwidth is calculated by the pathloss between MU and DBS i and the required data rate.

the altitude of DBS i will be adjusted to meet more MUs' data rate requirements. Specifically,

- 1) Denote h_i^* as the altitude of DBS i obtained from the **initial 3-D DBS placement**, and δ as the step size of adjusting the value of h_i^* , where $\delta^{\min} \leq \delta \leq \delta^{\max}$. Here, δ^{\min} and δ^{\max} are the minimum and maximum step size of δ , respectively. Initially, $\delta = \delta^{\min}$.
- 2) Adjust the altitudes of DBS i to be $h_i^- = \max(h_i^* - \delta, f^{\min}(x_i^d, y_i^d))$ and $h_i^+ = \min(h_i^* + \delta, f^{\max}(x_i^d, y_i^d))$, respectively. Calculate the number of MUs associated to DBS i (i.e., $\sum_{j \in J'} a_{ij}$) by re-executing **bandwidth allocation and MU association** based on the updated altitude of DBS i (i.e., h_i^- and h_i^+), respectively.
- 3) Denote $m(h_i^*)$, $m(h_i^+)$, and $m(h_i^-)$ as the number of the associated MUs when the altitude of DBS i is h_i^* , h_i^+ , and h_i^- , respectively. Here,

- If the adjusted altitudes of DBS i do not increase the number of associated MUs, then keep the original altitude of DBS i , i.e.,

$$h_i^* = h_i^*, \text{ if } m(h_i^*) \geq m(h_i^+) \ \& \ m(h_i^*) \geq m(h_i^-),$$

and adjust the step size $\delta = \delta + \delta^{\min}$.

- If the adjusted altitudes of DBS i increase the number of the associated MUs, then update the altitude of DBS i to be

$$h_i^* = \begin{cases} h_i^+, & \text{if } m(h_i^+) > m(h_i^*) \ \& \ m(h_i^+) \geq m(h_i^-), \\ h_i^-, & \text{if } m(h_i^-) > m(h_i^*) \ \& \ m(h_i^-) > m(h_i^+), \end{cases} \quad (24)$$

and $\delta = \delta^{\min}$.

Then, we will keep adjusting the altitudes of DBS i by going back to Step 2) in **altitude adjustment**. The altitude adjustment continues until $\delta > \delta^{\max}$.

Note that the RESCUE algorithm is periodically executed to update the DBS placement, bandwidth allocation, and MU association in order to accommodate the MU mobility.

The RESCUE algorithm comprises three processes, i.e., deriving the optimal 2-D location, altitude, and MU association and bandwidth allocation for all the DBSs. The time complexity of deriving the optimal 2-D location of a DBS (i.e., Steps 3-8 in Algorithm 1) is $O(|N||J|)$ (where $|N|$ and $|J|$ are the numbers of locations and MUs in the disaster struck area, respectively). The time complexity of deriving the optimal altitude and MU association of a DBS (i.e., Steps 9-22 in Algorithm 1) is $O(|J| + \frac{h^{\max} - h^{\min}}{\delta^{\min}})$ (where h^{\max} and h^{\min} are the highest and lowest altitude of the DBS for all locations, respectively). Therefore, the time complexity of RESCUE is $O(|I|(|N||J| + |J| + \frac{h^{\max} - h^{\min}}{\delta^{\min}})) = O(|I||N||J| + |I|\frac{h^{\max} - h^{\min}}{\delta^{\min}})$ (where $|I|$ is the number of DBSs).

The space complexity (i.e., the required memory space) of RESCUE is determined by the required memory for storing the MU movement matrix (which indicates the locations of all MUs in different time slots) and MU information matrix (which imposes the data rate requirements of the MUs). The space complexity of the MU movement and that of the MU information matrix are $O(|I||N|)$ and $O(|J|)$, respectively. Thus, the space complexity of RESCUE is $O(|I||N| + |J|)$.

Algorithm 1 RESCUE

- 1: Divide the disaster struck area into a number of locations with the same size.
- 2: **for** each DBS $i \in I$ **do**
- 3: **for** each location $n \in N$ **do**
- 4: Place DBS i over location n .
- 5: Calculate the optimal altitude of DBS i over location n , denoted as h_n , based on $f^{\max}(x_i^d, y_i^d)$, $f^{\min}(x_i^d, y_i^d)$, and Definition 2.
- 6: Calculate the number of MUs covered by DBS i , i.e., $|K_{in}|$.
- 7: **end for**
- 8: Calculate the optimal location for DBS i , i.e., n^* , where $n_i^* = \arg \max \{|K_{in}| \mid n \in N\}$. Denote h_i^* as the optimal altitude of DBS i once deployed over location n^* .
- 9: Construct an array by sorting all the MUs covered by DBS i in ascending order according to their bandwidth requirements b_{ij} (where $\forall j \in K_{in^*}$).
- 10: Iteratively select an MU in the array, allocate the amount of bandwidth (which equals to the MU's bandwidth requirement) to the MU, associate the MU to DBS i , and update the available bandwidth of DBS i (i.e., B_i). The iteration continues until all the MUs covered by DBS i are associated to DBS i , or DBS i does not have enough bandwidth to meet the bandwidth requirement of the selected MU, or the overall data rate between the associated MUs and DBS i exceeds the capacity of the FSO backhaul link between DBS i and its connected MBS.
- 11: Initialize the step size $\delta = \delta^{\min}$.
- 12: **while** $\delta \leq \delta^{\max}$ **do**
- 13: $h_i^- = \max(h_i^* - \delta, f^{\min}(x_i^d, y_i^d))$.
- 14: $h_i^+ = \min(h_i^* + \delta, f^{\max}(x_i^d, y_i^d))$.
- 15: Execute bandwidth allocation and MU association (i.e., Step 10) once the altitude of DBS i is h_i^- and h_i^+ , respectively.
- 16: Calculate $m(h_i^*)$, $m(h_i^+)$, and $m(h_i^-)$.
- 17: **if** $m(h_i^+) > m(h_i^*)$ and $m(h_i^+) > m(h_i^-)$ **then**
- 18: $\delta = \delta + \delta^{\min}$.
- 19: **else**
- 20: Update h_i^* based on Eq. (24).
- 21: **end if**
- 22: **end while**
- 23: **end for**

VI. SIMULATION RESULTS

In order to validate the performance of RESCUE, we conduct extensive simulations to compare the performance of RESCUE with two other baseline algorithms, i.e., traffic load aware DBS configuration (TLA) [40] and pathloss aware DBS configuration (PLA) [41]. The basic idea of TLA is to maximize the overall data rate between DBSs and MUs by first allocating bandwidth to the MUs with lower pathloss to their associated DBSs. However, TLA does not yield the optimal DBS deployment, and thus the locations of DBSs,

TABLE II
SIMULATION PARAMETERS

FSO transmission power (P_t)	200 mWatt
Divergence angle (θ_g)	1 mrad
Receiver radius (r)	0.05 m
Receiver sensitivity (N_b)	100 photons/bit
FSO wavelength (λ)	1550 nm
Visible distance v	10 km
Available MBS/DBS	4
Disaster area radius	2 km
Maximum altitude of DBS (f^{max})	200 m
Carrier frequency (f_c)	2 GHz
Environment index (b)	9.61 [42]
Environment index (β)	0.16 [42]
Average excessive pathloss in LoS (ξ^{LoS})	1 dB
Average excessive pathloss in NLoS (ξ^{NLoS})	20 dB
Noise power spectral density (N_0)	-104 dBm/Hz
DBS downlink transmission power	20 dBm
Available bandwidth for each DBS (B_i)	5 MHz

derived from RESCUE, will be applied to TLA. That is, TLA and RESCUE have the same DBS deployment but apply different access link bandwidth allocation methods. The basic idea of PLA is to jointly optimize the bandwidth allocation and horizontal locations of DBSs in order to minimize the average pathloss between MUs and their associated DBSs. However, the altitudes of DBSs are fixed and predefined. Here, we assume that if PLA determines to deploy DBS i over location (x_i^d, y_i^d) , then the altitude of the DBS is the minimum altitude to achieve LoS between the drone and its working base station, i.e., $f^{min}(x_i^d, y_i^d)$.

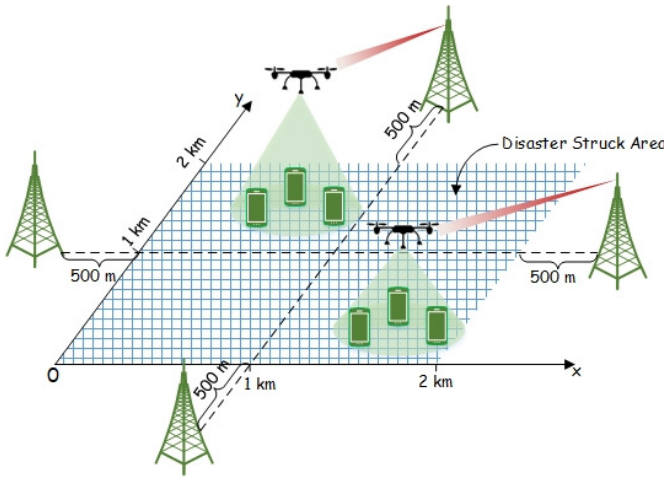


Fig. 3. Simulation setups.

The simulation is set up as follows: the size of the disaster struck area is 2×2 km. The disaster struck area is further divided into 100×100 small locations with the same size of 20×20 m. There are 4 working MBSs around the disaster struck area. The locations of these working MBSs are depicted in Fig. 3. The distribution of MUs in the disaster struck area follows a 2-D Poisson distribution with the average MU density equal to 20 MUs/location. The pathloss requirements of all MUs are the same, i.e., $\eta^{th} = 110$ dB. Also, the data rate requirements of MUs are generated based on the normal distribution with the mean and standard deviation equal to 3

Mbps and 1 Mbps, respectively. Other simulation parameters are shown in Table II.

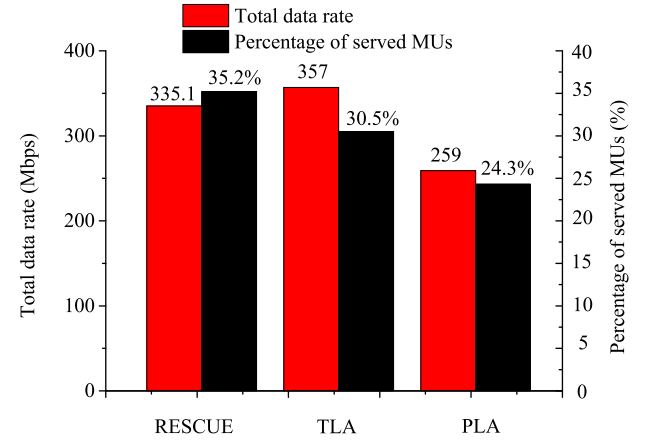


Fig. 4. Fraction of served MUs and total data rate incurred by different methods.

Fig. 4 shows the total data rate (i.e., the aggregated data rate of all MUs) and the fraction of served MUs incurred by the three algorithms. Here, the fraction of served MUs equals to the number of MUs with satisfied data rate requirements, divided by the total number of MUs in the disaster struck area. From the figure, we can see that RESCUE achieves the highest fraction of served MUs as compared to TLA and PLA; however, the total data rate incurred by RESCUE is lower than that incurred by TLA because RESCUE tries to maximize the number of served MUs, and so it prefers to allocate bandwidth to MUs, which require less bandwidth to meet their data rate requirements. On the other hand, TLA tries to maximize the overall data rate of MUs, and so it prefers to allocate bandwidth to MUs, which have the lower pathloss to their DBSs. Also, PLA incurs the worst performance in terms of the total data rate and the fraction of served MUs because PLA does not optimize the altitude of DBSs, thus degrading its performance accordingly.

Fig. 5 shows the cumulative distribution of served MUs' data rate requirements for the three methods; RESCUE has more than 60% of served MUs with data rate requirements no larger than 2.75 Mbps; however, TLA only has less than 30% of served MUs with data rate requirements no larger than 2.75 Mbps. The result demonstrates that RESCUE prefers to allocate bandwidth to the MUs which require less bandwidth to meet their data rate requirements.

Fig. 6 and Fig. 7 show the the fraction of served MUs and the total data rate by varying the average MU density of the area, respectively. RESCUE always incurs the highest fraction of served MUs, and TLA always incurs the highest total data rate of MUs. However, as the average MU density of the area increases, the difference of the total data rate incurred by RESCUE and TLA diminishes.

Next, we will analyze how the number of available DBSs affects the network performance. Note that the total amount of bandwidth assigned to these DBSs are fixed, and so more available DBSs means less amount of bandwidth assigned

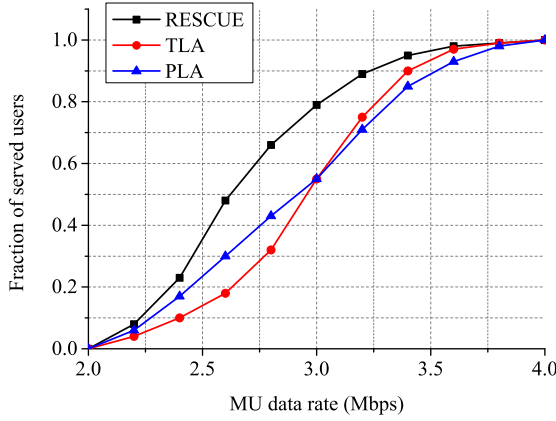


Fig. 5. Cumulative distribution of served MUs with different data rate requirement.

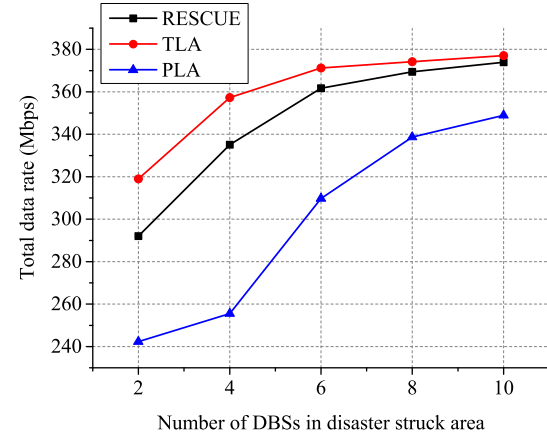


Fig. 8. Total data rate over different number of DBSs.

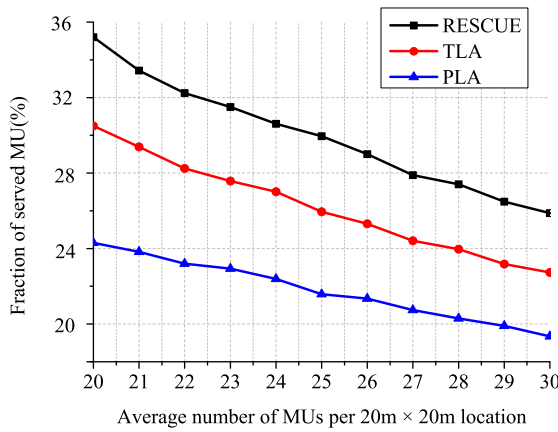


Fig. 6. Fraction of served MUs' data rate requirements.

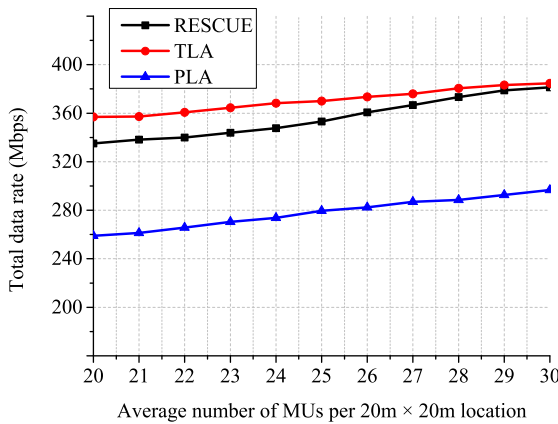


Fig. 7. Total data rate over different MU density.

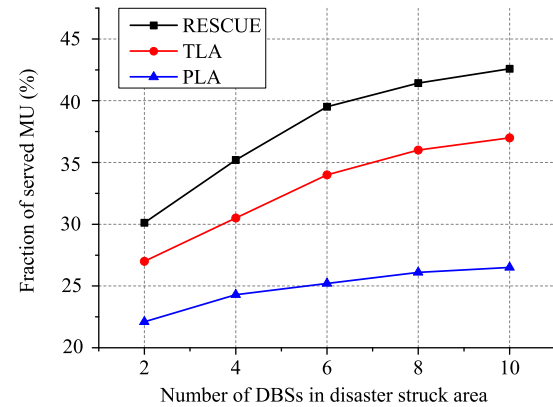


Fig. 9. Fraction of served MUs by varying the number of DBSs.

to each DBS. Fig. 8 and Fig. 9 show the total data rate and the fraction of served MUs by varying the number of available DBSs, respectively. Still, RESCUE achieves the

highest fraction of served MUs and TLA achieves the highest total data rate. Meanwhile, the difference between the total data rate incurred by RESCUE and the one incurred by TLA reduces because as the number of deployed DBSs increases, the average pathloss between a DBS and an MU reduces, and so the MUs which are served by RESCUE (to allocate bandwidth in order to meet their data rate requirements) have the higher probability of having lower pathloss to their DBSs. That is, the MUs selected by RESCUE have a higher probability of also being selected by TLA as the number of deployed DBSs increases. In addition, the performance of PLA is still the worst since it does not optimize the altitude of DBSs, thus resulting in a higher pathloss between MUs and their DBSs.

VII. CONCLUSIONS

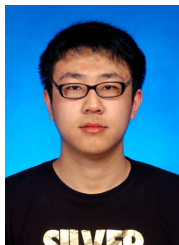
In this paper, we have proposed an FSO-based drone assisted mobile access network by deploying DBSs over the disaster struck area (where the network infrastructures and power supplies are destroyed) in order to provision network

connectivity to MUs. We have designed the RESCUE algorithm to jointly optimize the 3-D locations of the available DBSs, bandwidth allocation, and user association problem in order to maximize the number of MUs with guaranteed data rate requirements. Extensive simulations have been conducted to demonstrate the performance of RESCUE as compared to two other baseline algorithms.

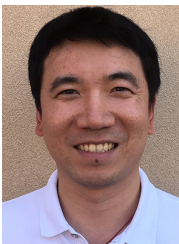
REFERENCES

- [1] X. Sun and N. Ansari, "Edgeiot: Mobile edge computing for the internet of things," *IEEE Communications Magazine*, vol. 54, no. 12, pp. 22–29, December 2016.
- [2] Ericsson, "Ericsson mobility report." [Online]. Available: <https://www.ericsson.com/assets/local/mobility-report/documents/2018/ericsson-mobility-report-november-2018.pdf>.
- [3] P. Rawat, M. Haddad, and E. Altman, "Towards efficient disaster management: 5G and device to device communication," in *2015 2nd International Conference on Information and Communication Technologies for Disaster Management (ICT-DM)*, Nov 2015, pp. 79–87.
- [4] C. Lee, "Wireless information and power transfer for communication recovery in disaster areas," in *Proceeding of IEEE International Symposium on a World of Wireless, Mobile and Multimedia Networks 2014*, June 2014, pp. 1–4.
- [5] D. Wu and N. Ansari, "High capacity spectrum allocation for multiple d2d users reusing downlink spectrum in lte," in *2018 IEEE International Conference on Communications (ICC)*, May 2018, pp. 1–6.
- [6] X. Guo, R. Nkrow, N. Ansari, L. Li, and L. Wang, "Robust wifi localization by fusing derivative fingerprints of rss and multiple classifiers," *IEEE Transactions on Industrial Informatics*, pp. 1–1, 2019.
- [7] K. Mase, "Communication service continuity under a large-scale disaster: Providing a wireless multihop network and shelter communication service for a disaster area under the great east japan earthquake," in *2012 IEEE International Conference on Communications (ICC)*, June 2012, pp. 6314–6318.
- [8] M. Narang, W. Liu, J. Gutierrez, and L. Chiaraviglio, "A cyber physical buses-and-drones mobile edge infrastructure for large scale disaster emergency communications," in *2017 IEEE 37th International Conference on Distributed Computing Systems Workshops (ICDCSW)*, June 2017, pp. 53–60.
- [9] T. Sakano, S. Kotabe, T. Komukai, T. Kumagai, Y. Shimizu, A. Takahara, T. Ngo, Z. M. Fadlullah, H. Nishiyama, and N. Kato, "Bringing movable and deployable networks to disaster areas: development and field test of mdru," *IEEE Network*, vol. 30, no. 1, pp. 86–91, January 2016.
- [10] Y. Lu, W. Wang, and B. Bhargava, "Hierarchical structure for supporting movable base stations in wireless networks," in *10th International Conference on Telecommunications, 2003. ICT 2003.*, vol. 1, Feb 2003, pp. 729–736 vol.1.
- [11] D. Wu, X. Sun, and N. Ansari, "A cooperative drone assisted mobile access network for disaster emergency communications," in *GLOBECOM 2019 - 2019 IEEE Global Communications Conference*, Dec 2019, accepted.
- [12] P. Li, T. Miyazaki, K. Wang, S. Guo, and W. Zhuang, "Vehicle-assist resilient information and network system for disaster management," *IEEE Transactions on Emerging Topics in Computing*, vol. 5, no. 3, pp. 438–448, July 2017.
- [13] Y. Xie, X. Liu, L. Kong, F. Wu, G. Chen, and A. V. Vasilakos, "Drone-based wireless relay using online tensor update," in *2016 IEEE 22nd International Conference on Parallel and Distributed Systems (ICPADS)*, Dec 2016, pp. 48–55.
- [14] X. Sun and N. Ansari, "Latency aware drone base station placement in heterogeneous networks," in *GLOBECOM 2017 - 2017 IEEE Global Communications Conference*, Dec 2017, pp. 1–6.
- [15] N. Ansari and X. Sun, "Mobile edge computing empowers internet of things," *IEICE Trans. Commun.*, vol. 101, no. 3, pp. 604–619, 2018.
- [16] A. Fotouhi, M. Ding, and M. Hassan, "Flying drone base stations for macro hotspots," *IEEE Access*, vol. 6, pp. 19 530–19 539, 2018.
- [17] X. Liu and N. Ansari, "Resource allocation in UAV-assisted M2M communications for disaster rescue," *IEEE Wireless Communications Letters*, vol. 8, no. 2, pp. 580–583, April 2019.
- [18] L. Zhang and N. Ansari, "On the number and 3-D placement of in-band full-duplex enabled drone-mounted base-stations," *IEEE Wireless Communications Letters*, vol. 8, no. 1, pp. 221–224, Feb 2019.
- [19] A. Al-Hourani, S. Kandeepan, and S. Lardner, "Optimal LAP altitude for maximum coverage," *IEEE Wireless Communications Letters*, vol. 3, no. 6, pp. 569–572, Dec 2014.
- [20] B. Galkin, J. Kibilda, and L. A. DaSilva, "Backhaul for low-altitude UAVs in urban environments," in *2018 IEEE International Conference on Communications (ICC)*, May 2018, pp. 1–6.
- [21] S. Liu, Z. Wei, Z. Guo, X. Yuan, and Z. Feng, "Performance analysis of UAVs assisted data collection in wireless sensor network," in *2018 IEEE 87th Vehicular Technology Conference (VTC Spring)*, June 2018, pp. 1–5.
- [22] A. Chaaban, J. Morvan, and M. Alouini, "Free-space optical communications: Capacity bounds, approximations, and a new sphere-packing perspective," *IEEE Transactions on Communications*, vol. 64, no. 3, pp. 1176–1191, March 2016.
- [23] Z. Zhao, Z. Zhang, J. Tan, Y. Liu, and J. Liu, "200 Gb/s FSO WDM communication system empowered by multiwavelength directly modulated TOSA for 5G wireless networks," *IEEE Photonics Journal*, vol. 10, no. 4, pp. 1–8, Aug 2018.
- [24] N. Cvijetic, D. Qian, J. Yu, Y. Huang, and T. Wang, "100 Gb/s per-channel free-space optical transmission with coherent detection and MIMO processing," in *2009 35th European Conference on Optical Communication*, Sept 2009, pp. 1–2.
- [25] X. Sun and N. Ansari, "Jointly optimizing drone-mounted base station placement and user association in heterogeneous networks," in *2018 IEEE International Conference on Communications (ICC)*, May 2018, pp. 1–6.
- [26] R. I. Bor-Yaliniz, A. El-Keyi, and H. Yanikomeroglu, "Efficient 3-D placement of an aerial base station in next generation cellular networks," in *2016 IEEE International Conference on Communications (ICC)*, May 2016, pp. 1–5.
- [27] S. Zhang, X. Sun, and N. Ansari, "Placing multiple drone base stations in hotspots," in *2018 IEEE 39th Sarnoff Symposium*, Sep. 2018, pp. 1–6.
- [28] M. Erdelj, E. Natalizio, K. R. Chowdhury, and I. F. Akyildiz, "Help from the sky: Leveraging UAVs for disaster management," *IEEE Pervasive Computing*, vol. 16, no. 1, pp. 24–32, Jan 2017.
- [29] S. Rahman, G. Kim, Y. Cho, and A. Khan, "Positioning of UAVs for throughput maximization in software-defined disaster area UAV communication networks," *Journal of Communications and Networks*, vol. 20, no. 5, pp. 452–463, Oct 2018.
- [30] A. M. Hayajneh, S. A. R. Zaidi, D. C. McLernon, M. D. Renzo, and M. Ghogho, "Performance analysis of UAV enabled disaster recovery networks: A stochastic geometric framework based on cluster processes," *IEEE Access*, vol. 6, pp. 26 215–26 230, 2018.
- [31] W. Fawaz, C. Abou-Rjeily, and C. Assi, "UAV-aided cooperation for FSO communication systems," *IEEE Communications Magazine*, vol. 56, no. 1, pp. 70–75, Jan 2018.
- [32] M. Alzenad, M. Z. Shakir, H. Yanikomeroglu, and M. Alouini, "FSO-based vertical backhaul/fronthaul framework for 5G+ wireless networks," *IEEE Communications Magazine*, vol. 56, no. 1, pp. 218–224, Jan 2018.
- [33] Z. Gu, J. Zhang, Y. Ji, L. Bai, and X. Sun, "Network topology reconfiguration for FSO-based fronthaul/backhaul in 5G+ wireless networks," *IEEE Access*, vol. 6, pp. 69 426–69 437, 2018.
- [34] M. Najafi, H. Ajam, V. Jamali, P. D. Diamantoulakis, G. K. Karagiannis, and R. Schober, "Statistical modeling of FSO fronthaul channel for drone-based networks," in *2018 IEEE International Conference on Communications (ICC)*, May 2018, pp. 1–7.
- [35] A. Al-Hourani, S. Kandeepan, and S. Lardner, "Optimal LAP altitude for maximum coverage," *IEEE Wireless Communications Letters*, vol. 3, no. 6, pp. 569–572, Dec 2014.
- [36] E. Kalantari, H. Yanikomeroglu, and A. Yongacoglu, "On the number and 3D placement of drone base stations in wireless cellular networks," in *2016 IEEE 84th Vehicular Technology Conference (VTC-Fall)*, Sept 2016, pp. 1–6.
- [37] H. Falaki, D. Lymberopoulos, R. Mahajan, S. Kandula, and D. Estrin, "A first look at traffic on smartphones," in *Proceedings of the 10th ACM SIGCOMM conference on Internet measurement.* ACM, 2010, pp. 281–287.
- [38] M. Alzenad, M. Z. Shakir, H. Yanikomeroglu, and M. Alouini, "FSO-Based vertical backhaul/fronthaul framework for 5G+ wireless networks," *IEEE Communications Magazine*, vol. 56, no. 1, pp. 218–224, Jan 2018.
- [39] S. Singh and G. Soni, "Pointing error evaluation in FSO link," in *Fifth International Conference on Advances in Recent Technologies in Communication and Computing (ARTCom 2013)*, Sept 2013, pp. 365–370.

- [40] N. N. Bhuiyan, R. T. Ratri, I. Anjum, and M. A. Razzaque, "Traffic-load aware spectrum allocation in cloud assisted cognitive radio networks," in *2017 IEEE Region 10 Humanitarian Technology Conference (R10-HTC)*, Dec 2017, pp. 598–601.
- [41] J. Cho and J. Kim, "Performance comparison of heuristic algorithms for UAV deployment with low power consumption," in *2018 International Conference on Information and Communication Technology Convergence (ICTC)*, Oct 2018, pp. 1067–1069.
- [42] W. Shi, J. Li, W. Xu, H. Zhou, N. Zhang, S. Zhang, and X. Shen, "Multiple drone-cell deployment analyses and optimization in drone assisted radio access networks," *IEEE Access*, vol. 6, pp. 12 518–12 529, 2018.

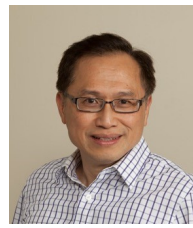


Di Wu [S'17] received his B.E. degree in communication engineering and his M.E. degree in information and communication engineering from Harbin Institute of Technology, China. He is currently working toward his Ph.D. degree in electrical engineering at the New Jersey Institute of Technology (NJIT), Newark. His research interests include mobile edge computing, network security, and resource management in fog computing.



Xiang Sun [S'13, M'18] is Assistant Professor of Electrical and Computer Engineering at the University of New Mexico. He received the B.E. and M.E. degrees from the Hebei University of Engineering in 2008 and 2011, respectively, and the Ph.D. degree in electrical engineering from the New Jersey Institute of Technology (NJIT) in 2018. He has (co-)authored 26 technical publications, held one U.S. patent, and filed six U.S./PCT non-provisional patent applications. His research interests include mobile edge computing, cloud computing, Internet

of Things, wireless networks, big-data-driven networking, and green communications and computing. He has also served as a TPC member of many conferences. He has received several honors and awards, including the 2016 IEEE International Conference on Communications Best Paper Award, the 2017 IEEE Communications Letters Exemplary Reviewers Award, the 2018 NJIT Hashimoto Price, the 2018 Inter Digital Innovation Award on IoT Semantic Mashup, the 2019 NJIT Outstanding Doctoral Dissertation Award, and the 2019 IEICE Communications Society Best Tutorial Paper Award. He is currently an Associate Editor of Digital Communications and Networks.



Nirwan Ansari [S'78, M'83, SM'94, F'09] received a Ph.D. from Purdue University, an MSEE from the University of Michigan, and a BSEE (summa cum laude with a perfect GPA) from the New Jersey Institute of Technology (NJIT). He is Distinguished Professor of Electrical and Computer Engineering at NJIT.

He authored *Green Mobile Networks: A Networking Perspective* (Wiley-IEEE, 2017) with T. Han, and co-authored two other books. He has also (co-)authored more than 600 technical publications, over 280 published in widely cited journals/magazines. He has guest-edited a number of special issues covering various emerging topics in communications and networking. He has served on the editorial/advisory board of over ten journals including as Associate Editor-in-Chief of IEEE Wireless Communications Magazine. His current research focuses on green communications and networking, cloud computing, drone-assisted networking, and various aspects of broadband networks.

He was elected to serve in the IEEE Communications Society (ComSoc) Board of Governors as a member-at-large, has chaired some ComSoc technical and steering committees, has been serving in many committees such as the IEEE Fellow Committee, and has been actively organizing numerous IEEE International Conferences/Symposia/Workshops. He is frequently invited to deliver keynote addresses, distinguished lectures, tutorials, and invited talks. Some of his recognitions include several Excellence in Teaching Awards, a few best paper awards, the NCE Excellence in Research Award, the ComSoc TC-CSR Distinguished Technical Achievement Award, the ComSoc AHSN TC Technical Recognition Award, the IEEE TCGCC Distinguished Technical Achievement Recognition Award, the NJ Inventors Hall of Fame Inventor of the Year Award, the Thomas Alva Edison Patent Award, Purdue University Outstanding Electrical and Computer Engineering Award, the NCE 100 Medal, and designation as a COMSOC Distinguished Lecturer. He has also been granted more than 40 U.S. patents.